New Antiferromagnetic Dinuclear Complexes of Nickel(II) with Two Azides as Bridging Ligands. Magneto–Structural Correlations

Joan Ribas,*[1a] Montserrat Monfort,[1a] Carmen Diaz,[1a] Carles Bastos,[1a] and Xavier Solans[1b]

Departament de Química Inorgànica, Universitat de Barcelona, Diagonal 647, 08028-Barcelona, Spain, and Departament de Cristal.lografia i Mineralogia, Universitat de Barcelona, Martí i Franqués s/n, 08028-Barcelona, Spain

Received December 29, 1992

Three new nickel(II) dinuclear azide-bridged compounds, $(\mu_{1,3}\text{-}N_3)_2[Ni(en)_2]_2(PF_6)_2$ (**1**), $(\mu_{1,3}\text{-}N_3)_2[Ni(1,3\text{-}pn)_2]_2[B(C_6H_5)_4]_2$ (**2**), and $(\mu_{1,3}\text{-}N_3)_2[Ni(1,2\text{-}pn)]_2(PF_6)_2$ (**3**), have been synthesized and characterized (en = ethylenediamine; 1,3-pn = 1,3-diaminopropane; 1,2-pn = 1,2-diaminopropane). The crystal structures of **1** and **2** have been solved. Complex **1** crystallizes in the monoclinic system, space group $C2/c$, with fw = 731.79, a = 15.252(3) Å, b = 17.872(3) Å, c = 12.102(2) Å, β = 126.76(2)°, V = 2643(1) Å^3, Z = 4, R = 0.053, and R_w = 0.057. Complex **2** crystallizes in the monoclinic system, space group $P2_1/n$, with fw = 1136.4, a = 9.997(2) Å, b = 20.838(3) Å, c = 14.269(3) Å, β = 96.76(2)°, V = 2952(2) Å^3, Z = 2, R = 0.052, and R_w = 0.052. In both complexes the nickel atom is placed in a distorted octahedral environment. The magnetic properties of these compounds have been studied by means of susceptibility measurements vs temperature. The χ_M vs T plots for **1**–**3** show the typical shapes for antiferromagnetically coupled nickel(II) dinuclear complexes. By using the spin Hamiltonian $-JS_1S_2$, J values for **1**–**3** were calculated to be –4.6, –114.5, and –77.2 cm^{-1}, respectively. Extended Hückel calculations on the two structurally characterized complexes, compared with two other analogous complexes previously reported in the literature, indicate that the dihedral angle between the N–Ni–N plane and the plane formed by the two N_3^- bridging ligands is the main factor which dominates the magnetic coupling: the smaller the dihedral angle, the stronger the antiferromagnetic coupling.

Introduction

The azido anion is a versatile bridging ligand which can coordinate Ni(II) ions giving dinuclear complexes in either end-to-end[2–4] or end-on[5–7] form, tetranuclear complexes in end-on[8] form, 1-D complexes in end-to-end form (uniform chains[9–11] and alternating chains[12]), and, finally, bidimensional complexes in which are present both end-to-end and end-on forms.[13] Regarding specifically the reported dinuclear complexes with end-to-end azide bonding, only four structurally characterized complexes are described in the literature.[2–4] One of them presents only one single azido bridge,[2] another two present double azido bridges,[3,4] and the fourth has three bridging azido ligands.[4] The first complex[2] can be considered as the smallest fragment or precursor of polynuclear 1-D Ni(II) complexes with a single azido bridge.[9–11] In all cases, 1,3-coordination gives antiferromagnetic behavior and 1,1-coordination gives ferromagnetic coupling. These results agree with the spin polarization theory, previously reported by Kahn and co-workers for azido derivatives of the Cu(II) ion.[14] Focusing our attention on dinuclear systems with double azido bridges, we realized that there is a significant difference in the J values reported in the literature (from –47.5 to –90.0 cm^{-1}).[3,4] Bencini et al.[15] have studied magneto–structural correlations in dinuclear Co(II) complexes with end-to-end azido bridges and tried to rationalize the same effect for Ni(II) compounds. In order to develop these correlations, we have synthesized new dinuclear species with two N_3^- bridges using several bidentate amines as blocking ligands for each Ni(II). Here we present the synthesis, characterization, and magnetic studies of three new dinuclear complexes of Ni(II) with double azido bridges. Once more, all these 1,3 complexes are antiferromagnetically coupled. The structures of two of them have been fully solved. With these two structures, together with those previously reported in the literature, we have interpreted the different magnetic behaviors by correlating them with structural parameters. Only one parameter has a relevant difference in these structures: the dihedral angle δ defined as the angle between the $(N_3)_2$ (least-squares) plane and the N–Ni–N plane. This dihedral angle varies between 0 and 45°.

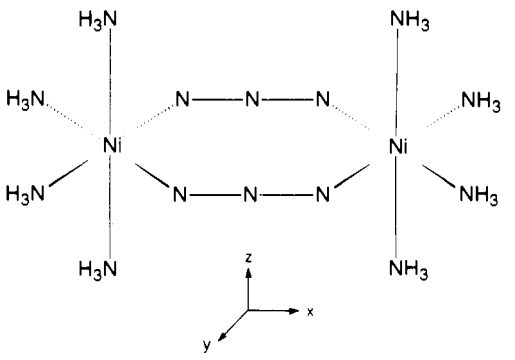

(1) (a) Department of Inorganic Chemistry. (b) Department of Crystallography.
(2) Wagner, F.; Mocella, M. T.; D'Aniello, M. J.; Wang, A. J. H.; Barefield, E. K. *J. Am. Chem. Soc.* **1974**, *96*, 2625.
(3) Pierpont, C. G.; Hendrickson, D. N.; Duggan, D. M.; Wagner, F.; Barefield, E. K. *Inorg. Chem.* **1975**, *14*, 604.
(4) Chaudhuri, P.; Guttman, M.; Ventur, D.; Wieghardt, K.; Nuber, B.; Weiss, J. J. *J. Chem. Soc., Chem. Commun.* **1985**, 1618.
(5) Arriortua, M. I.; Cortés, A. R.; Lezama, L.; Rojo, T.; Solans, X. *Inorg. Chim. Acta* **1990**, *174*, 263.
(6) Escuer, A.; Vicente, R.; Ribas, J. *J. Magn. Magn. Mater.* **1992**, *110*, 181.
(7) Cortés, R.; Ruis de Larramendi, J. I.; Lezama, L.; Rojo, T.; Urtiaga, K.; Arriortua, M. I. *J. Chem. Soc., Dalton Trans.* **1992**, 2723.
(8) Ribas, J.; Monfort, M.; Costa, R.; Solans, X. *Inorg. Chem.* **1993**, *32*, 695.
(9) Vicente, R.; Escuer, A.; Ribas, J.; El Fallah, M. S.; Solans, X. *Inorg. Chem.* **1993**, *32*, 1033.
(10) Gadet, V.; Verdaguer, M.; Renard, J. P.; Ribas, J.; Monfort, M.; Diaz, C.; Solans, X.; Landee, C. P.; Lamet, J. P.; Dworkin, A. *J. Am. Chem. Soc.*, in press.
(11) Escuer, A.; Vicente, R.; Ribas, J.; El Fallah, M. S.; Solans, X.; Font-Bardía, M. *Inorg. Chem.*, in press.
(12) Vicente, R.; Escuer, A.; Ribas, J.; Solans, X. *Inorg. Chem.* **1992**, *31*, 1726.
(13) Monfort, M.; Ribas, J.; Solans, X. *J. Chem. Soc., Chem. Commun.* **1993**, 350.
(14) Charlot, M. F.; Kahn, O.; Chaillet, M.; Larrieu, C. *J. Am. Chem. Soc.* **1986**, *108*, 2574 and references therein.
(15) Bencini, A.; Ghilardi, C. A.; Midollini, S.; Orlandini, A. *Inorg. Chem.* **1989**, *28*, 1958.

0020-1669/93/1332-3557$04.00/0

All other structural parameters (distances and angles) are very similar for all complexes. Extended Huckel calculations varying this parameter showed the great importance of this angle in the overlap of the magnetic orbitals and, indeed, in the J parameter. A similar result was noted by Kahn for bis(μ-hydroxo)dicopper(II) complexes,[16] and a related result was observed by Sinn[17] and discussed by Hodgson.[18]

Experimental Section

Caution! Azide complexes of metal ions are potentially explosive. Only a small amount of material should be prepared, and it should be handled with caution.

Synthesis of the New Complexes. The three complexes were prepared in similar ways: To an aqueous solution of 1 mmol (0.290 g) of $Ni(NO_3)_2 \cdot 6H_2O$ and 2 mmol of the corresponding amine (en = 0.12 g; 1,3-pn = 0.15 g; 1,2-pn = 0.15 g) was added an aqueous solution of 1 mmol (0.065 g) of NaN_3. After filtration to remove any impurity, 1.1 mmol of the corresponding counteranion (0.185 g of KPF_6 for **1** and **3** and 0.376 g of $Na[B(C_6H_5)_4]$ for **2**) was added. The aqueous solutions for **1** and **3** were left undisturbed, and well-shaped dark blue crystals of **1** were obtained after several days; all attempts to obtain single crystals of **3** were unsuccessful. Only microcrystals were obtained. Upon the addition of $Na[B(C_6H_5)_4]$ to the solution with 1,3-pn, a pale blue precipitate immediately formed. Once filtered off and washed with cold water, it was redissolved in acetonitrile. After several days, blue-violet single crystals of **2** were obtained. Satisfactory analytical results (C, H, N, Ni) were obtained for all complexes.

Physical Measurements. Magnetic measurements were carried out on polycrystalline samples with a pendulum-type magnetometer (MANICS DSM8) equipped with a helium continuous-flow cryostat, working in the temperature range 300–4 K, and a Bruker BE15 electromagnet. The magnetic field was approximately 15 000 G. For all compounds, the independence of the magnetic susceptibility versus the applied field was checked at room temperature up to 1.8 T. The instrument was calibrated by a magnetization measurement of a standard ferrite. Diamagnetic corrections were estimated from Pascal's constants.

Crystal Data Collection and Refinement. Crystals of **1** (0.08 × 0.08 × 0.15) and **2** (0.1 × 0.1 × 0.2 mm) were selected and mounted on an Enraf-Nonius CAD4 four-circle diffractometer. Unit cell parameters were determined from automatic centering of 25 reflections ($12 \le \theta \le 16°$ for **1** and $16 \le \theta \le 21°$ for **2**) and refined by least-squares methods. Intensities were collected with graphite-monochromatized Mo Kα radiation, using the $\omega/2\theta$ scan technique. For **1**, 2544 reflections were measured in the range $2 \le \theta \le 25°$, 1633 of which were assumed as observed by applying the condition $I \ge 2.5\sigma(I)$. For **2**, 4437 reflections were measured in the range $2 \le \theta \le 30°$, 3979 of which were assumed as observed by applying the same condition. In both compounds three reflections were measured every 2 h as orientation and intensity controls, significant intensity decay was not observed. Lorentz–polarization corrections but not absorption corrections were made. The crystallographic data are shown in Table I. The crystal structures were solved by Patterson synthesis using the SHELXS computer program[19] and refined by full-matrix least-squares methods, using the SHELX76[20] computer programs. The function minimized was $\sum w[|F_o| - |F_c|]^2$ where $w = [\sigma^2(F_o) + k|F_o|^2]^{-1}$ and $k = 0.0021$ for **1** and 0.0 for **2**. f, f', and f'' were taken from ref 21. The positions of all H atoms were computed and refined with an overall isotropic temperature factor, using a riding model. For **1**, the final R factor was 0.053 ($R_w = 0.057$) for all observed reflections. The number of parameters refined was 211. Maximum shift/esd = 0.1; maximum and minimum peaks in the final difference synthesis were 0.3 and –0.3 e Å^{-3}, respectively. For **2**, the final R factor was 0.052 (R_w = 0.052) for all observed reflections. The number of parameters refined was 353. Maximum shift/esd = 0.1. Maximum and minimum peaks in the final difference synthesis were again 0.3 and –0.3 e Å^{-3}, respectively. Final atomic coordinates for **1** and **2** are given in Tables II and III, respectively.

Table I. Crystallographic Data for $(\mu_{1,3}\text{-}N_3)_2[Ni(en)_2]_2(PF_6)_2$ (**1**) and $(\mu_{1,3}\text{-}N_3)_2[Ni(1,3\text{-}pn)_2]_2[B(C_6H_5)_4]_2$ (**2**)

	1	**2**
formula	$C_8H_{32}F_{12}N_{14}Ni_2P_2$	$C_{60}H_{80}B_2N_{14}Ni_2$
fw	731.7	1136.4
temp, K	298	298
space group	$C2/c$	$P2_1/n$
a, Å	15.252(3)	9.997(2)
b, Å	17.872(3)	20.838(3)
c, Å	12.102(2)	14.269(3)
β, deg	126.76(2)	96.76(2)
V, Å^3	2643(1)	2952(2)
Z	4	2
λ(Mo Kα), Å	0.710 69	0.710 69
d_{calc}, g·cm^{-3}	1.839	1.287
μ(Mo Kα), cm^{-1}	16.64	6.91
R^a	0.053	0.052
$R_w{}^b$	0.057	0.052

$^a \sum||F_o| - |F_c||/\sum|F_o|$. $^b R_w = [\sum w(|F_o| - |F_c|)^2/\sum w|F_o|^2]^{1/2}$.

Table II. Final Atomic Coordinates (×10^4; Ni, ×10^5) and Equivalent Isotropic Thermal Parameters (Å^2) and Their Estimated Standard Deviations for $(\mu\text{-}N_3)_2[Ni(en)_2]_2(PF_6)_2$

	x/a	y/b	z/c	$B_{eq}{}^a$
Ni	83242(7)	6344(5)	79799(9)	2.19(4)
N(1)	8619(5)	5(4)	9717(7)	3.39(30)
N(2)	9293(5)	–467(3)	10262(6)	2.30(24)
N(3)	9946(5)	–933(4)	10812(7)	3.65(30)
N(4)	8595(5)	–340(3)	7250(7)	3.01(28)
N(5)	6693(5)	261(4)	6741(7)	3.49(31)
N(6)	8112(5)	1580(3)	8775(7)	3.31(30)
N(7)	8074(5)	1380(3)	6464(6)	2.93(28)
C(1)	7621(7)	–818(4)	6641(9)	4.16(42)
C(2)	6621(6)	–333(5)	5865(9)	4.38(40)
C(3)	8180(8)	2235(4)	8072(10)	4.67(47)
C(4)	7604(7)	2070(4)	6585(9)	3.91(40)
P(1)	5000	1221(2)	2500	3.30(12)
P(2)	5000	–2278(2)	2500	4.01(16)
F(1)	5000	340(4)	2500	5.87(39)
F(2)	5000	2110(4)	2500	5.88(44)
F(3)	4728(5)	1216(3)	1017(5)	5.68(29)
F(4)	3730(4)	1220(3)	1821(6)	5.46(27)
F(5)	6174(24)	–2433(21)	3656(32)	13.60(210)
F(6)	5315(17)	–2865(13)	1752(21)	7.26(113)
F(7)	4665(25)	1739(12)	8158(27)	6.59(133)
F(5)′	10370(63)	3517(20)	12298(73)	7.15(251)
F(6)′	10258(27)	2733(35)	11490(37)	8.59(233)
F(7)′	10137(34)	1927(19)	12202(42)	7.15(206)
F(5)″	8783(12)	2758(15)	11151(18)	6.63(87)

$^a B_{EQ} = 8\pi^2/3\sum_i\sum_j U_{ij}a^*_i a^*_j A_i A_j$.

Results and Discussion

Description of the Structures. $(\mu_{1,3}\text{-}N_3)_2[Ni(en)_2]_2(PF_6)_2$ (1). The unit cell contains four dinuclear [NiNi] dications and eight hexafluorophosphate anions. Selected bond lengths and angles are listed in Table IV. Other distances and angles may be found in the supplementary material. A view of the dinuclear unit with the atom-labeling scheme is presented in Figure 1. The nickel atom occupies a distorted octahedral environment. The central core, $Ni(N_3)_2Ni$, important from a magnetic point of view, has an inversion center with two Ni–N(N_3) distances of 2.181 and 2.183 Å. The N–Ni–N angles are 90.6°, and the N–N–Ni angles are 121.1 and 119.3°, respectively. The dihedral angle δ, as defined in the Introduction, is 45°, creating a chairlike structure.

$(\mu_{1,3}\text{-}N_3)_2[Ni(1,3\text{-}pn)_2]_2[B(C_6H_5)_4]_2$ (2). The unit cell contains two dinuclear [NiNi] dications and four tetraphenylborate anions. Main bond lengths and angles are listed in Table V. Other distances and angles will be found in the supplementary material. A view of the dinuclear unit with the atom-labeling scheme is

(16) (a) Charlot, M. F.; Jeannin, S.; Jeannin, Y.; Kahn, O.; Lucrece-Abaul, J.; Martin-Frere, J. *Inorg. Chem.* **1979**, *18*, 1675. (b) Charlot, M. F.; Kahn, O.; Jeannin, S.; Jeannin, Y. *Inorg. Chem.* **1980**, *19*, 1410.
(17) Butcher, R. J.; Sinn, E. *Inorg. Chem.* **1976**, *15*, 1604.
(18) Hodgson, D. J. *Inorg. Chem.* **1976**, *12*, 3174.
(19) Sheldrick, G. M. *Acta Crystallogr.* **1990**, *A46*, 467.
(20) Sheldrick, G. M. SHELX. A computer program for crystal structure determination. University of Cambridge, England, 1976.
(21) *International Tables for X-ray Crystallography*; Kynoch Press: Birmingham, England, 1976.

Table III. Final Atomic Coordinates (×10⁴; Ni, ×10⁵) and Equivalent Isotropic Thermal Parameters (Å²) and Their Estimated Standard Deviations for $(\mu\text{-}N_3)_2[Ni(1,3\text{-pn})_2]_2[B(C_6H_5)_4]_2$

	x/a	y/b	z/c	B_{EQ}[a]
Ni	13013(6)	6681(3)	14448(5)	3.18(3)
B	3484(6)	1177(2)	7247(4)	3.26(25)
N(1)	1640(4)	-277(2)	885(3)	3.39(19)
N(2)	990(4)	-544(2)	279(3)	3.23(19)
N(3)	-364(5)	829(2)	380(3)	4.34(23)
N(4)	956(4)	1630(2)	1834(3)	3.58(19)
N(5)	2587(4)	959(2)	504(3)	4.40(23)
N(6)	38(4)	267(2)	2354(3)	3.75(21)
N(7)	2938(4)	494(2)	2468(3)	4.02(22)
C(1)	1973(6)	2137(3)	1799(4)	5.02(31)
C(2)	2476(6)	2130(3)	845(4)	5.16(32)
C(3)	3486(6)	1559(3)	704(5)	5.47(33)
C(4)	107(7)	423(3)	3351(5)	5.75(35)
C(5)	1672(6)	265(3)	3823(5)	5.37(33)
C(6)	2812(6)	664(3)	3478(4)	5.22(31)
C(7)	3645(5)	404(2)	7584(4)	3.41(23)
C(8)	3369(5)	-87(2)	6954(4)	3.84(25)
C(9)	3264(6)	-743(3)	7236(4)	5.07(32)
C(10)	3457(6)	-879(3)	8181(5)	5.13(32)
C(11)	3763(6)	-419(3)	8910(4)	4.84(30)
C(12)	3839(6)	235(2)	8563(4)	4.33(26)
C(13)	1923(5)	1300(2)	7155(3)	3.31(22)
C(14)	1072(5)	1235(2)	6303(4)	3.83(25)
C(15)	-306(6)	1318(3)	6219(5)	5.37(33)
C(16)	-1053(6)	1419(3)	6992(4)	4.65(29)
C(17)	-194(6)	1483(3)	7852(5)	5.16(32)
C(18)	1183(6)	1413(3)	7925(4)	4.67(30)
C(19)	4212(5)	1314(2)	6299(4)	3.65(24)
C(20)	3775(5)	1883(2)	5751(4)	4.07(26)
C(21)	4442(6)	2063(3)	4989(4)	4.88(30)
C(22)	5418(6)	1677(3)	4652(4)	4.99(31)
C(23)	5846(6)	1114(3)	5216(4)	4.37(28)
C(24)	5167(5)	954(2)	5938(4)	4.23(27)
C(25)	4356(5)	1670(2)	8037(4)	3.68(24)
C(26)	3780(5)	2263(2)	8224(4)	3.61(24)
C(27)	4598(6)	2699(3)	8835(4)	4.71(30)
C(28)	5786(6)	2522(3)	9305(4)	4.59(29)
C(29)	6361(6)	1933(3)	9124(4)	4.53(28)
C(30)	5562(6)	1519(3)	8486(4)	4.47(28)

[a] $B_{EQ} = 8\pi^2/3\sum_i\sum_j U_{ij}a^*_i a^*_j a_i a_j$.

Table IV. Main Bond Lengths (Å) and Angles (deg) for $(\mu_{1,3}\text{-}N_3)_2[Ni(en)_2]_2(PF_6)_2$

N(1)–Ni	2.181(6)	N(3)–N(2)	1.156(8)
N(4)–Ni	2.103(6)	C(1)–N(4)	1.473(9)
N(5)–Ni	2.102(6)	C(2)–N(5)	1.458(10)
N(6)–Ni	2.065(6)	C(3)–N(6)	1.487(9)
N(7)–Ni	2.109(6)	C(4)–N(7)	1.478(9)
N(3)I–Ni	2.183(6)	C(2)–C(1)	1.498(12)
N(2)–N(1)	1.178(8)	C(4)–C(3)	1.485(12)
N(4)–Ni–N(1)	89.9(2)	N(3)–N(2)–N(1)	178.6(7)
N(5)–Ni–N(1)	89.8(2)	N(3)[a]–Ni–N(6)	87.2(2)
N(5)–Ni–N(4)	83.3(2)	N(3)[a]–Ni–N(7)	86.9(2)
N(6)–Ni–N(1)	88.4(3)	N(2)–N(1)–Ni	121.1(5)
N(6)–Ni–N(4)	177.7(3)	N(2)[a]–N(3)–Ni[a]	119.3(5)
N(6)–Ni–N(5)	98.2(3)	C(1)–N(4)–Ni	107.3(4)
N(7)–Ni–N(1)	171.9(2)	C(2)–N(5)–Ni	107.0(5)
N(7)–Ni–N(4)	97.9(2)	C(3)–N(6)–Ni	107.1(5)
N(7)–Ni–N(5)	93.4(2)	C(4)–N(7)–Ni	106.7(4)
N(7)–Ni–N(6)	83.7(2)	C(2)–C(1)–N(4)	108.8(6)
N(3)[a]–Ni–N(1)	90.6(2)	C(1)–C(2)–N(5)	111.1(7)
N(3)[a]–Ni–N(4)	91.2(2)	C(4)–C(3)–N(6)	110.1(7)
N(3)[a]–Ni–N(5)	174.5(2)	C(3)–C(4)–N(7)	108.4(6)

[a] Symmetry code: $-x, -y, -z$.

presented in Figure 2. The Ni atom occupies a distorted octahedral environment. The central core, $Ni(N_3)_2Ni$, important from a magnetic point of view, has an inversion center with two Ni–N(N_3) distances of 2.167 and 2.144 Å. The N–Ni–N angles are 91.5°, and the N–N–Ni angles are 127.7 and 139.0°, respectively. The dihedral angle δ, as defined in the Introduction, is 3°, giving a nearly planar structure.

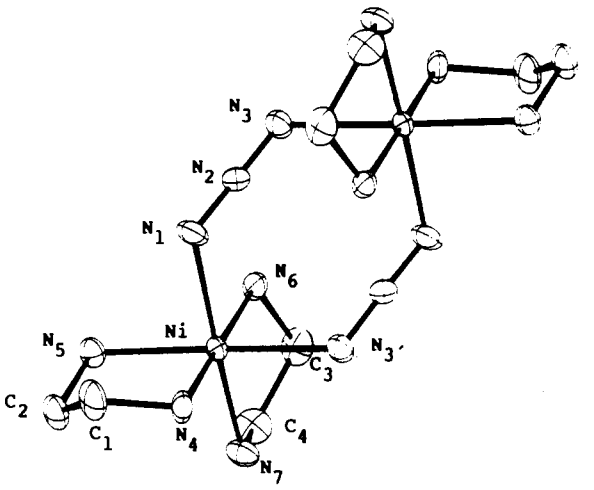

Figure 1. Molecular structure for $(\mu_{1,3}\text{-}N_3)_2[Ni(en)_2]_2(PF_6)_2$ (**1**) showing the atom-labeling scheme.

Table V. Main Bond Lengths (Å) and Angles (deg) for $(\mu_{1,3}\text{-}N_3)_2[Ni(1,3\text{-pn})_2]_2[B(C_6H_5)_4]_2$

N(1)–Ni	2.167(4)	C(1)–N(4)	1.472(6)
N(3)–Ni	2.144(5)	C(3)–N(5)	1.547(7)
N(4)–Ni	2.120(4)	C(4)–N(6)	1.453(7)
N(5)–Ni	2.056(4)	C(6)–N(7)	1.504(7)
N(6)–Ni	2.089(4)	C(2)–C(1)	1.506(8)
N(7)–Ni	2.092(4)	C(3)–C(2)	1.589(8)
N(2)–N(1)	1.161(5)	C(5)–C(4)	1.662(8)
N(3)[a]–N(2)	1.221(5)	C(6)–C(5)	1.538(8)
N(3)–Ni–N(1)	91.3(1)	N(6)–Ni–N(5)	173.5(2)
N(4)–Ni–N(1)	173.6(2)	N(7)–Ni–N(1)	87.5(1)
C(5)–C(6)–N(7)	109.1(4)	N(7)–Ni–N(3)	178.8(2)
N(2)–N(1)–Ni	127.7(3)	N(7)–Ni–N(4)	96.9(1)
N(3)[a]–N(2)–N(1)	176.7(4)	N(7)–Ni–N(5)	90.5(2)
N(2)–N(3)–Ni[a]	139.0(3)	N(7)–Ni–N(6)	88.7(2)
C(5)–C(4)–N(6)	106.6(5)	C(1)–N(4)–Ni	122.4(3)
C(6)–C(5)–C(4)	117.5(5)	C(3)–N(5)–Ni	120.8(3)
N(4)–Ni–N(3)	84.3(2)	C(4)–N(6)–Ni	123.8(3)
N(5)–Ni–N(1)	83.7(2)	C(6)–N(7)–Ni	118.8(3)
N(5)–Ni–N(3)	89.1(2)	C(2)–C(1)–N(4)	109.3(5)
N(5)–Ni–N(4)	91.5(2)	C(3)–C(2)–C(1)	114.0(5)
N(6)–Ni–N(1)	89.8(1)	C(2)–C(3)–N(5)	105.4(4)
N(6)–Ni–N(3)	91.5(2)		
N(6)–Ni–N(4)	95.0(1)		

[a] Symmetry code: $-x, -y, -z$.

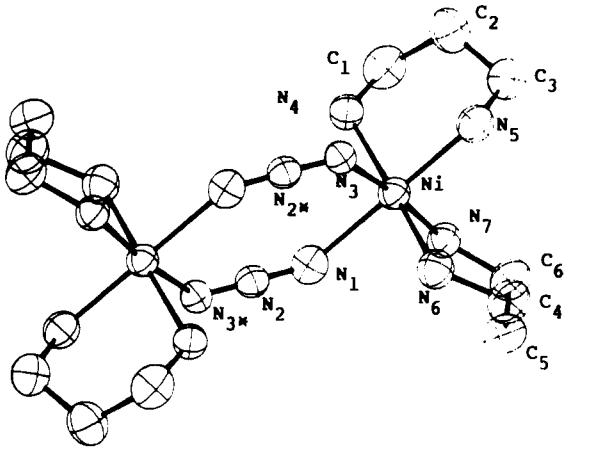

Figure 2. Molecular structure for $(\mu_{1,3}\text{-}N_3)_2[Ni(1,3\text{-pn})_2]_2[B(C_6H_5)_4]_2$ (**2**) showing the atom-labeling scheme.

Magnetic Properties. The χ_M vs T plots for complexes **1**–**3** are shown in Figure 3. The χ_M values first increase, reaching a maximum at ≈ 6 K for **1**, at 168 K for **2**, and at 110 K for **3**, and then decrease. This behavior is typical of an antiferromagnetically coupled $Ni^{II}Ni^{II}$ pair. Variable-temperature suscep-

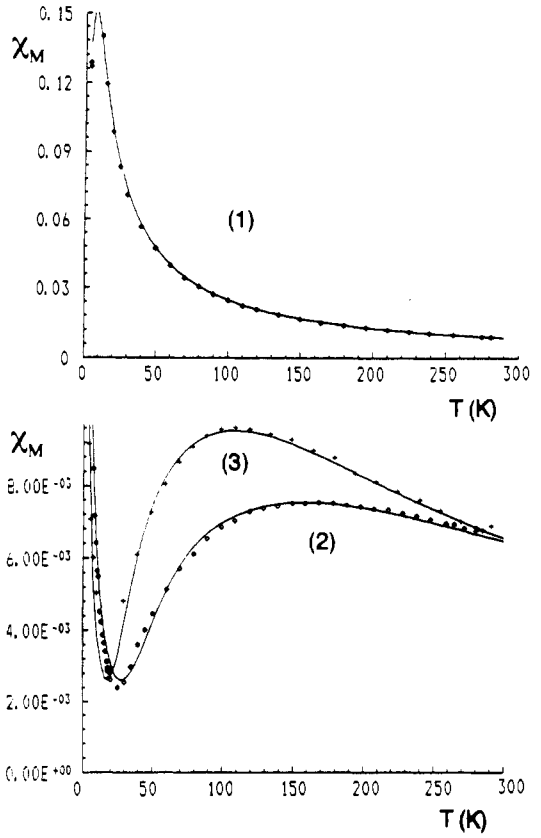

Figure 3. Experimental and calculated (—) temperature dependence of χ_M (cm^3 mol^{-1}) for the dinuclear compounds $(\mu_{1,3}\text{-}N_3)_2[Ni(en)_2](PF_6)_2$ (**1**), $(\mu_{1,3}\text{-}N_3)_2[Ni(1,3\text{-}pn)_2]_2[B(C_6H_5)_4]_2$ (**2**), and $(\mu_{1,3}\text{-}N_3)_2[Ni(1,2\text{-}pn)_2]_2(ClO_4)_2$ (**3**).

tibility data (4–300 K) for **1–3** were analyzed using the isotropic Heisenberg model[22] with $H = -JS_1S_2$, assuming a zero-field parameter $D = 0$. Least-squares fitting of the magnetic data leads to the following parameters: $J = -4.6$ cm^{-1}, $g = 2.3$, and τ (paramagnetic impurities) = 0.5% for **1**; $J = -114.5$ cm^{-1}, $g = 2.4$, and $\tau = 2.8\%$ for **2**; and $J = -77.2$ cm^{-1}, $g = 2.3$, and $\tau = 2.9\%$ for **3**. The minimized function was $R = \sum(\chi_M^{calcd} - \chi_M^{obs})^2/\sum(\chi_M^{obs})^2$, and in the three cases R was less than 10^{-4}. Taking into account these results, our hypothesis ($D = 0$) may be correct for **2** and **3** owing to their great J values. For **1**, the small J value indicates the need to improve the fitting by considering the D parameter.[23] Applying the Ginsberg formula,[23] J slightly decreases (ca. -3 cm^{-1}) but in the best fitting an anomalously large D parameter (>10 cm^{-1}) is found which, as already indicated by Ginsberg,[23] strongly correlates with $z'J'$ (interdimer interactions). Thus, it is impossible to calculate accurately the D and $z'J'$ values. In fact, both effects are present in our complexes at low temperature. For this reason, and taking into consideration that the J value varies only slightly (from ca. -4 to ca. -3 cm^{-1}), there is not significant variation in the results for $D = 0$. J values show that the overlap between the magnetic orbitals is efficient in **2** and **3** but very inefficient in **1** (J almost negligible). In order to establish magneto–structural correlations, one must consider the main magnetic and structural data for all complexes with two azido bridging ligands, shown in Table VI. From a structural point of view, we can observe that the parameter which shows greatest variation is the dihedral angle δ (as defined in the Introduction), whereas the distances Ni–N and all other angles show only minor variations. Taking this into account, an attempt was made to correlate the J variation (from -4 to -114 cm^{-1}) with this parameter.

(22) O'Connor, C. J. *Prog. Inorg. Chem.* **1982**, *29*, 239.
(23) Ginsberg, A. P.; Martin, R. L.; Brookes, R. W.; Sherwood, R. C. *Inorg. Chem.* **1972**, *11*, 2884.

Table VI. Magnetic (J, cm^{-1}) and Structural Parameters (Distances, Å; angles, deg) for Dinuclear $(\mu_{1,3}\text{-}N_3)_2$ Complexes

compd	J	Ni–N	N–Ni–N	N–N–Ni	dihedral	ref
1	−4.6	2.181	90.6	119.3	45.0	*d*
		2.183		121.1		
2	−114.5	2.167	91.3	127.7	3.0	*d*
		2.144		139.0		
3	−77.2					*d*
4[a]	−70	2.069	91.7	123.3	20.7	3
		2.195		135.7		
5[b]	−90	2.168	92.4	124.4	6.8	4
		2.135		138.4		
6[c]	−47					4

[a] With L = tren. [b] With L = 1,5,9-triazacyclododecane. [c] With L = 1,4,7-trimethyl-1,4,7-triazacyclononane. [d] This work.

MO Calculations. To verify this explanation, extended Hückel MO calculations were performed on the structurally characterized dinuclear complexes using the CACAO program.[24] The atomic parameters used for Ni, N, and H were the standards of the program.

According to Table VI, there are three possible variable parameters with which magneto–structural correlations could be found: distances Ni–N(azide), which are generally asymmetric; angles N–N–Ni, also asymmetric; and the dihedral angle δ between the $(N_3)_2$ (least-squares) plane and the N(1)–Ni–N(2) plane. In all cases, there is an inversion center in the middle of the completely planar $(N_3)_2$ plane, and the angle N–Ni–N is close to 90°.

In order to center this analysis on the coordination environment of the nickel(II) cations, according to the four structural examples available, the geometry was modeled as

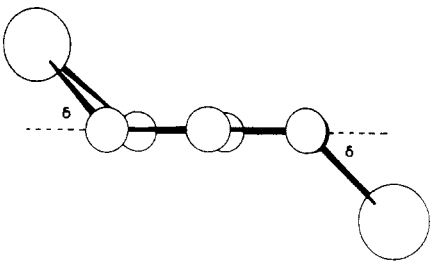

placing the nickel atoms in a slightly distorted octahedral environment. The angle N–Ni–N was taken as 90°, and the bond distances Ni–N(NH_3) as 2.10 Å and Ni–N(azide) as 2.16 Å. From a structural point of view, if we suppose a perfectly symmetric and planar structure (dihedral angle δ equal to zero and all angles and distances equivalent), the angles N–N–Ni should be 135°. If we bend the structure (by varying the dihedral angle δ from 0 to 90°), the N–N–Ni angles should vary from 135 to 90°. Indeed, compound **1**, with a dihedral angle of 45° has all Ni–N distances equal and the four N–N–Ni angles very close to 120°. In contrast, in the two almost planar complexes, **2** and **5**, the average N–N–Ni angles are between 133.3 and 131.6°, very close to the theoretical 135°. This small difference could be attributed to the asymmetry of the Ni–N distances (see Table VI).

For this reason we have performed extended Hückel calculations on the idealized molecule shown above, allowing the two Ni(II) atoms to rotate freely around the two terminal N atoms of the two azide bridging ligands, to study the influence of the variation of the dihedral angle δ on the magnetic coupling between both metallic centers.

For a dimeric nickel(II) system with two unpaired electrons on each metal atom, four molecular orbitals φ_1, φ_2, φ_3, and φ_4 (φ_1 and φ_2 with z^2 and φ_3 and φ_4 with xy as the main contribution) are expected. In fact, the Walsh diagram for these four significant

(24) Mealli, C.; Proserpio, D. M. *J. Chem. Educ.* **1990**, *67*, 3399.

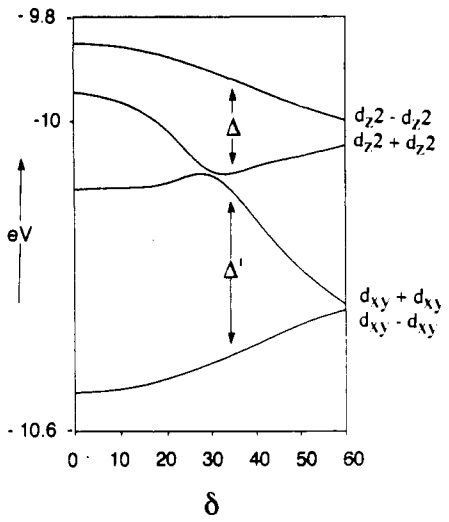

Figure 4. Walsh diagram for the four combinations of magnetic orbitals upon variation of the dihedral angle, δ, as defined in the Introduction.

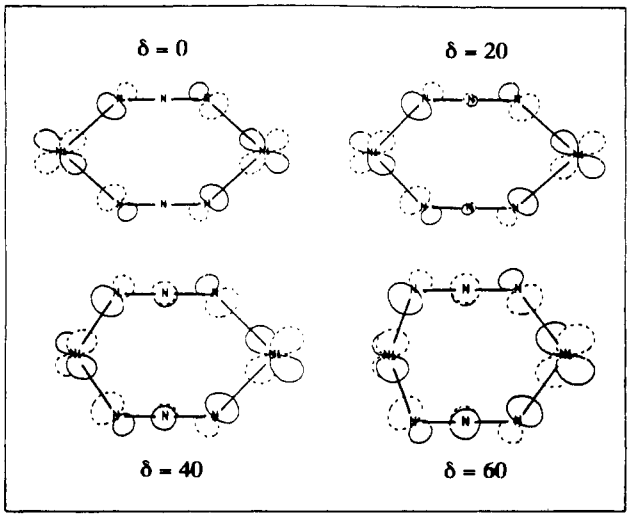

Figure 5. Dependence of the overlap between the two molecular orbital fragments (FMO) $d_{xy} + d_{xy}$ and $2N_3$ on the dihedral angle δ. For simplicity only four steps (δ = 0, 20, 40, 60°) are drawn. In all cases, the two azido bridge ligands are maintained in the *xy* plane.

orbitals when the dihedral angle δ varies from 0 to 60° (larger values seem to be sterically hindered) is shown in Figure 4. The first MO is the antisymmetric combination of d_{z^2} orbitals with the corresponding p orbitals of the two azide bridging ligands. This antibonding MO is slightly stabilized when the dihedral angle δ is increased from 0 to 60° due to an increase in the p character of the two central N atoms and a decrease in the terminal N atoms, giving a less antibonding character. The second MO is the antisymmetric combination of d_{xy} Ni(II) orbitals with the corresponding p orbitals of the two bridging azides. There is a very pronounced stabilization of this antibonding orbital when the dihedral angle, δ, increases from 0 to 60°. This stabilization is due to a decrease in the p_x,p_y hybrid character in the four N terminal atoms of the azide bridge, perfectly oriented on the d_{xy} orbitals of Ni(II) for δ equal to 0° but less oriented when the δ angle is increased (Figure 5), simultaneously occurring with the increase in the p character of the two central N atoms when δ is increased (Figure 5). This situation creates a reduction in the antibonding character of the MO, stabilizing its energy. Finally, the two symmetric combinations, $z^2 + z^2$ and $xy - xy$ (Figure 4), show a different behavior: the overlap between the corresponding orbitals of Ni(II) and those deriving from the N_3^- fragments is less effective at 0° than at 60°, which increases the antibonding character.

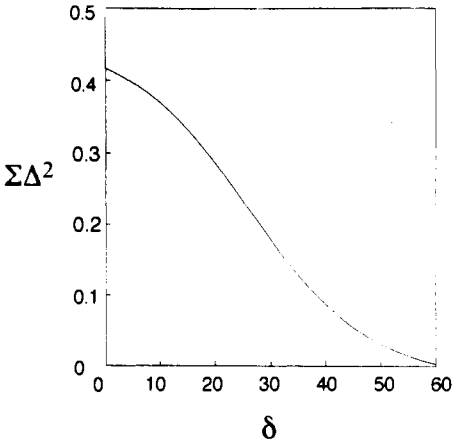

Figure 6. Variation of $\Sigma\Delta^2$ as a function of the dihedral angle δ.

For this Ni_2 system with spin states $S = 0$, 1, and 2, $E_2 - E_1 = -4J$ and $E_1 - E_0 = -2J$, in which $4J = K - V$. K is a ferromagnetic term, generally very small, derived from bielectronic integrals, and V is an antiferromagnetic term, which can be described[25] as a function of the splitting of the pairs of molecular orbitals as follows:

$$V = {}^1/_2(\mathcal{E}_1 - \mathcal{E}_2)^2/(J_{aa} - J_{ac}) + {}^1/_2(\mathcal{E}_3 - \mathcal{E}_4)^2/(J_{bb} - J_{bd})$$

where $\mathcal{E}_i$ are the energies of the d orbitals (1, 2 for d_{xy} and 3, 4 for d_{z^2}) and J_{mn} are bielectronic integrals, all assumed to be constant in a series of complexes of similar geometries.

Consequently, J_{af} can be assumed to be proportional to the sum of the square of the gaps between MO's of the same symmetry (z^2 and xy respectively). In Figure 6 we have represented this sum of the two gaps as a function of the dihedral angle δ. We can see that there is a large decrease in J value upon passing from dihedral angle 0° (maximum value) to 60° ($J \approx 0$). From the results gathered in Table VI, we can observe good agreement between experimental and theoretical values for all dihedral angles. For dihedral angles near 0°, J has maximum values (ca. $-114\ cm^{-1}$ for δ = 3° and ca. $-90\ cm^{-1}$ for δ = 7°); for intermediate δ angles (complex **4**), we observe an intermediate J value ($-70\ cm^{-1}$), and finally, for the greatest dihedral angle δ, J is almost negligible ($-4\ cm^{-1}$). To take into account the effect of the actual asymmetry of Ni–N distances and N–N–Ni angles, we carried out extended Hückel calculations on a planar structure (dihedral angle δ = 0°), varying the angles and distances in an asymmetrical form (maintaining the inversion center in all cases). The effect observed in the four "magnetic" orbitals is much less pronounced than that reported for the δ variation. A great distortion in angles and distances (not experimentally found in any of the studied complexes) would be necessary to be an important factor in the variation of magnetic behavior. Consequently, with all the reservations due kind of calculation, we can assume that the great difference in the magnetic behaviors of these dinuclear Ni(II) complexes can be related to the value of the dihedral angle δ between both Ni(II) and the plane of the two azide bridging ligands.

Acknowledgment. We are very grateful for financial assistance from the CICYT (Grant PB88-0197).

Supplementary Material Available: Tables giving crystal data and details of the structure determinations, anisotropic thermal parameters, hydrogen atom coordinates, and bond angles and distances for **1** and **2** (10 pages). Ordering information is given on any current masthead page.

(25) Hay, P. J.; Thibeault, J. C.; Hoffmann, R. *J. Am. Chem. Soc.* **1975**, *97*, 4884.